Identifying open-volume defects in doped and undoped perovskite-type $LaCoO_3$, $PbTiO_3$, and $BaTiO_3$

Vinita J. Ghosh and Bent Nielsen
Brookhaven National Laboratory, Upton, New York 11973

Thomas Friessnegg
University of Maryland, College Park, Maryland 20742
(Received 9 August 1999)

Dopants, vacancies, and impurity-vacancy clusters have a substantial impact on the properties of perovskite-type metal oxides (general formula ABO_3). In order to determine synthesis and processing conditions that optimize the desirable properties of these materials a careful study of these defects is required. It is essential to identify the defects and to map the defect densities. Positron annihilation spectroscopy has often been used to identify vacancy-type defects. Calculations of the positron lifetime and Doppler-broadened profiles of the positron-electron annihilation radiation in undoped and doped $LaCoO_3$, $PbTiO_3$, and $BaTiO_3$ are reported, and compared with available experimental data. The results show that these positron techniques are excellent for studying open-volume defects, vacancy-impurity complexes, and for identifying the sublattice occupied by the dopants.

INTRODUCTION

The many applications of perovskite-type oxide materials in electronics have drawn much attention in the past decade. These applications take advantage of the ferroelectric, pyroelectric, high permittivity, and piezoelectric properties of these materials for a variety of devices such as nonvolatile memories, high density dielectric memories, uncooled infrared detectors, as well as sensors, actuators, and electrodes.[1,2] Reliability and reproducibility are important issues in the fabrication of many of these devices. A guideline for improving reliability parameters such as fatigue, imprint, and retention is to control the defect density in the material. Although defect models for some bulk materials have been reported in the literature,[3–6] the precise defect structure in thin-film materials may be more complex and is not well understood. Improved defect characterization in bulk materials as well as thin films is therefore essential.

Positron annihilation spectroscopy (PAS) has become a valuable tool, used to characterize open-volume and substitutional defects in thin-film and bulk materials. Some of the numerous advantages of this technique are that it is nondestructive, that no special sample preparation is required, and that it has potential for *in situ* studies. In the past the PAS method has been extensively used to investigate defects in metals, semiconductors, and polymers.[7] However, little theoretical[8,9] and experimental[10–15] work has been done for bulk forms of metal oxides with a perovskite structure, and only recently has the PAS technique been applied to investigate thin films of these materials.[16–18]

In this paper we report on a systematic study of the positron annihilation characteristics in the perovskite-oxide materials $LaCoO_3$, $PbTiO_3$, and $BaTiO_3$. Positron lifetimes and Doppler profiles have been calculated for the defect-free bulk as well as for different lattice defects. These calculated values have been compared to existing experimental data. The effects of doping and lattice relaxations around a defect have also been investigated.

CALCULATION METHOD

Positron lifetime calculations have been done for a number of elemental materials,[19–22] for different open-volume defects in Si,[23,24] and for some La oxides.[8,9] Various calculation methods have been used, full band-structure calculations,[19,20] pseudopotential methods,[24] and atomic superposition methods.[8,9,21] The same calculation techniques (band-structure,[25,26] pseudopotential,[24] and atomic superposition methods[21,27–29]) have been used for the calculation of the Doppler profiles. It has been shown that band-structure calculations give better agreement with experimental data than atomic superposition methods for positron lifetimes,[19–21] as well as for Doppler profiles.[21] However, band-structure methods cannot easily be used for large supercells, and large supercells (consisting of hundreds of atoms) are required for studying defects in complex materials, especially metal oxides. The application of atomic superposition methods to positron lifetimes in metal oxides has yielded reasonably good agreement with experimental data.[8,9] Comparisons with experimental Doppler broadening data for elemental solids[27] show that the calculated profiles qualitatively reproduce all the features of the experimental data, even though the discrepancies between the calculated and measured values may be as large as a factor of two.[21] It should be kept in mind that the atomic superposition model fails to describe the delocalized valence states accurately, and that the calculated profiles are less accurate below $20\times10^{-3}m_0c$, where m_0 is the rest mass of the electron and c the velocity of light. The major contribution to the positron lifetimes is due to annihilations with valence electrons and therefore one would not expect good agreement with experimental data, but the calculated values in Refs. 8 and 9 show reasonably good agreement.

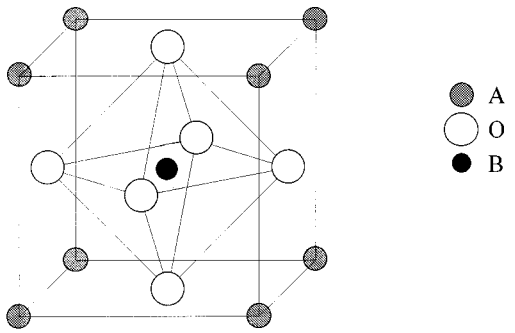

FIG. 1. The structure of perovskite-type metal oxides.

Another approximation inherent in these calculations is the simulation of charged ions by neutral atoms. These materials are likely to have sizable relaxations near vacancy-type defects, and the magnitude of these effects has to be calculated by some other methods. We have used shell-model calculations to estimate the magnitude of the relaxations, and then used these values to calculate the effects of these relaxations on the positron lifetimes.

We have used the atomic superposition method[21,28] for the calculation of the positron lifetimes and the Doppler broadening. Supercells with at least 135 atoms (often 320 or more atoms) were used for the calculations. Ratio curves (plotting the ratios of a Doppler profile to a reference profile) were used to highlight the differences between the profiles of materials with defects to defect-free materials. The positions, magnitudes, and shapes of the special features (peaks or valleys) can be used to identify vacancies or vacancy-impurity clusters. The impact of the detector resolution on the ratio curves is quite significant,[30] it may alter the position, magnitude, or the shape of the peaks that are used to identify the defects. It is important that the appropriate detector resolution is used in the calculations, and in comparing data from different experimental setups. A Gaussian detector resolution function with a full width at half maximum of 1.5 keV was convoluted with the calculated values to correspond to the experimental detector resolution.

RESULTS AND DISCUSSION

The three materials we studied are all perovskite-type metal oxides, with the general formula ABO_3. In the formula ABO_3, A represents the large cations, La, Pb, or Ba; and B the smaller cations Co or Ti. The atomic positions are shown in Fig. 1. The larger A ions occupy the eightfold coordinated site (0,0,0), B ions occupy the site (0.5,0.5,0.5), while the oxygens occupy the equipoints (0.5,0.5,0). $PbTiO_3$ and $BaTiO_3$ are ferroelectric perovskites. They have similar cohesive properties such as unit-cell volume, but different ferroelectric behavior, which has not been fully understood.[31] In addition to the cubic phase $BaTiO_3$ exists in the tetragonal, orthorhombic, and rhombohedral phases, whereas $PbTiO_3$ can also exist in the tetragonal phase. The ferroelectric distortions involve a displacement of the B sublattice with respect to the anion sublattice, resulting in a net dipole moment or polarization. For the purposes of the calculation we assume that the Ti occupies the symmetric bcc site. The lattice constants for the cubic phases in $PbTiO_3$ and $BaTiO_3$ are used for the calculations.[32,33] Undoped $LaCoO_3$ has a cubic structure but Sr doping introduces rhombohedral distortions proportional to the Sr content.[34] The lattice constant for the cubic phase of undoped $LaCoO_3$ is used in our calculations.

TABLE I. Positron lifetimes in the undoped perovskite-type metal oxides.

	Positron lifetimes (ps) in		
	$LaCoO_3$	$PbTiO_3$	$BaTiO_3$
Defect-free	129	147	152
V_A	275	280	293
V_B	173	175	204
V_O	145	152	162
$2V_O$	160		
$3V_O$	170		
V_AV_O	280	284	
V_AV_A	281		
V_AV_B	277		
V_BV_O	202		
$V_BV_OV_O$		252	

A. Positron lifetimes and Doppler-broadened profiles for undoped materials

Calculated values of the positron lifetimes in all three materials are listed in Table I. In all of these materials positron lifetimes associated with vacancies on different sublattices have very different values, and these lifetimes can be used to identify the defect site. Positrons annihilating at vacancies associated with the large cation sites (A) have longer lifetimes than those at the smaller cation sites (B). Lifetimes associated with oxygen vacancies are not much longer than positron lifetimes in defect-free materials. Positron lifetime experiments,[11–15] discussed in the next section, point to the existence of defect complexes with longer lifetimes. These complexes may be charge-neutral combinations of anion-cation vacancies, or clusters of oxygen vacancies. Positron lifetimes for annihilation at some vacancy clusters are also listed in Table I. As expected the positron lifetimes at vacancy complexes are larger than those at individual vacancies. They do not, however, appear to change dramatically as the cluster size increases.

The positron lifetime at vacancies is expected to change due to the relaxations of the ions surrounding the vacancy. These changes were briefly explored using shell-model calculations to estimate the magnitude of these relaxations. Shell-model calculations have been done to look at relaxations near oxygen vacancies in $YBa_2Cu_3O_7$.[35] These results show that the neighboring copper atoms move away from the vacancy, whereas the oxygen ions move towards the vacant site. The magnitude of these relaxations is typically around 10% of the interatomic spacing, and is of the same order as the observed structure changes in oxygen-deficient $YBa_2Cu_3O_7$.[36] Similar calculations for Y, Ba, and Cu vacancies[37] show that the relaxations associated with the large cation vacancies can be somewhat larger. We assumed similar relaxations around vacancies in $LaCoO_3$ and tried to estimate the impact of these relaxations on the values of the

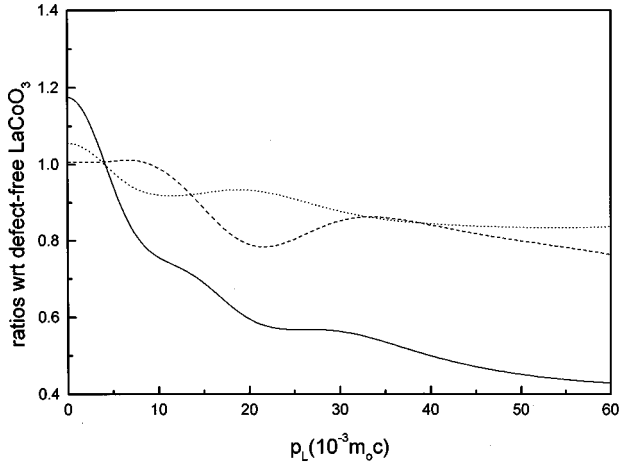

FIG. 2. Ratio curves of the La (solid line), Co (dashed line), and the O (dotted line) vacancies in $LaCoO_3$ with respect to defect-free $LaCoO_3$.

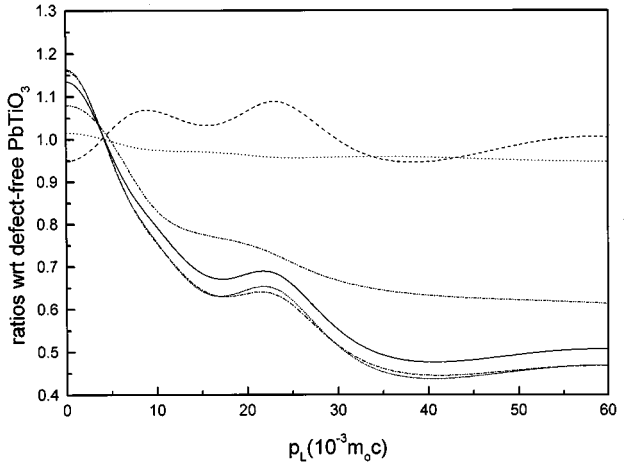

FIG. 3. Ratio curves for the simple vacancies V_{Pb} (solid line), V_{Ti} (dashed line), V_O (dotted line), and the $V_{Pb}V_O$ (dot-dash), $V_{Ti}2V_O$ (dot-dot-dashed), and the $2La_{Pb}V_{Pb}$ complexes (small dots) in $PbTiO_3$ with respect to defect-free $PbTiO_3$.

positron lifetime. For La vacancies in $LaCoO_3$ the vacancy-oxygen distance was increased by 10% and the vacancy-cobalt distance was decreased by 10%. The calculations predicted a small (10 ps) decrease in the positron lifetime. To study a Co vacancy the Co-O distance was increased by 10% and the Co-La distance was decreased 10%. This resulted in a larger decrease (30 ps) of the positron lifetime. For the oxygen vacancy the O-O distance was decreased (by 10%) and the O-La and O-Co distances were increased (by 10%). These relaxations increased the positron lifetime associated with the oxygen vacancies by about 30 ps. Since the structure of $YBa_2Cu_3O_7$ is more complex than that of the cubic perovskite oxides and relaxation effects near defects may have very different magnitudes. Therefore shell-model calculations should be performed for the metal oxides under study, and their impact on the positron lifetimes and Doppler broadening should be explored carefully.

The Doppler profiles of the materials we studied also exhibit some interesting features. Vacancies on different sublattices have distinguishable features, which can be used to identify the vacancy sublattice. Ratio curves for vacancies in $LaCoO_3$ with respect to defect-free $LaCoO_3$ are shown in Fig. 2, for vacancies in $PbTiO_3$ with respect to defect-free $PbTiO_3$ in Fig. 3, and for vacancies in $BaTiO_3$ with respect to defect-free $BaTiO_3$ in Fig. 4. The three figures show that vacancies on different sublattices have very different shapes, and these shapes can be used for identifying the defect site. Moreover, the signature peaks for defects on corresponding sublattices (*A*, *B*, or *O* sublattices) in the three perovskites have qualitatively the same features. Doppler profiles for some vacancy combinations were also calculated. Ratio curves for single vacancies and vacancy clusters in $PbTiO_3$ are plotted in Fig. 3. The ratio curve for a cluster consisting of a Pb and an O vacancy has features similar to a Pb vacancy. The charge-neutral combination of one Ti and two O vacancies, however, results in a ratio curve that is clearly distinguishable from either the Ti or the O vacancies. This difference in the shape of the signature peak may be due to the relaxations associated with this defect complex.

B. Influence of doping on positron lifetimes and Doppler-broadened profiles

It is believed that in Sr-doped $LaCoO_3$ the Sr ions occupy the La sites. When La^{3+} ions are replaced by Sr^{2+} ions the negative effective charge can be balanced either by the Co^{3+} ions changing to Co^{4+} (valence compensation), or by the creation of an oxygen vacancy (vacancy compensation) for every two Sr ions. To study the impact of the Sr doping a virtual crystal was created that was similar to $LaCoO_3$ but with all La atoms replaced by Sr atoms. The replacement of all La atoms by Sr atoms increased the positron lifetime from 129 ps (Table I) to 144 ps (Table II). The defect cluster with two Sr atoms on La sites complexed with an oxygen vacancy has a larger lifetime (160 ps) than the defect-free $LaCoO_3$ crystal (129 ps), or the isolated oxygen vacancy (145 ps).

Another way to determine which mechanism is responsible for the charge compensation is to look at the Doppler profiles. Figure 5 shows the change in the ratio curves as a function of the Sr concentration (valence compensation). The ratio curve for the defect complex consisting of two substitutional Sr atoms bound to an oxygen vacancy is also plotted

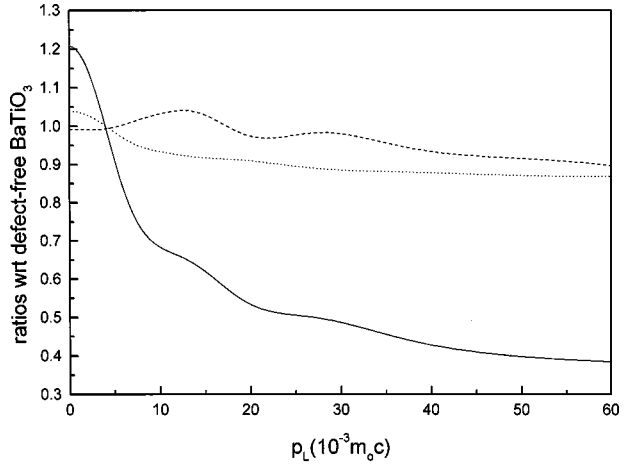

FIG. 4. Ratio curves for V_{Ba} (solid line), V_{Ti} (dashed line), and V_O (dotted line) in $BaTiO_3$ with respect to defect-free $BaTiO_3$.

TABLE II. Positron lifetimes for some ''hypothetical'' crystals and impurity-vacancy complexes in doped metal oxides.

	Positron lifetimes (ps)
$LaCoO_3$	129
$La_{0.85}Sr_{0.15}CoO_3$	134
$La_{0.67}Sr_{0.33}CoO_3$	140
$SrCoO_3$	144
$2Sr_{La}V_O$	160
$PbTiO_3$	147
$LaTiO_3$	136
$PbZrO_3$	141
$LaZrO_3$	132
$2La_{Pb}V_{Pb}$	278
$SrTiO_3$	164
$BaSrO_3$	149
$Sr_{Ti}V_O$	154

in Fig. 5. The shape of the ratio curve for this complex is found to be quite different from that of the virtual crystals with substitutional Sr or the isolated oxygen vacancy (Fig. 2) in $LaCoO_3$. The presence of the oxygen vacancy causes the positron to be localized near the substitutional Sr, and the signal can be interpreted as a combination of a La vacancy and a substitutional Sr.

When $PbTiO_3$ is doped with La the large La ion probably occupies the Pb site. Charge compensation during the substitution of Pb^{2+} by La^{3+} ions would probably result in a defect complex with two substitutional La ions (at Pb sites) bound to a Pb vacancy (vacancy compensation). Both the positron lifetime (Table I) and the Doppler profile (Fig. 3) of such a defect complex were found to be very similar to those of an isolated Pb vacancy.

To examine the maximum effect of substituting Pb with La atoms, or Ti by Zr atoms, we created hypothetical structures with the same lattice constant as $PbTiO_3$, by replacing all Pb atoms by La atoms (creating $LaTiO_3$), or by replacing Ti with Zr (creating $PbZrO_3$), or by simultaneously replacing

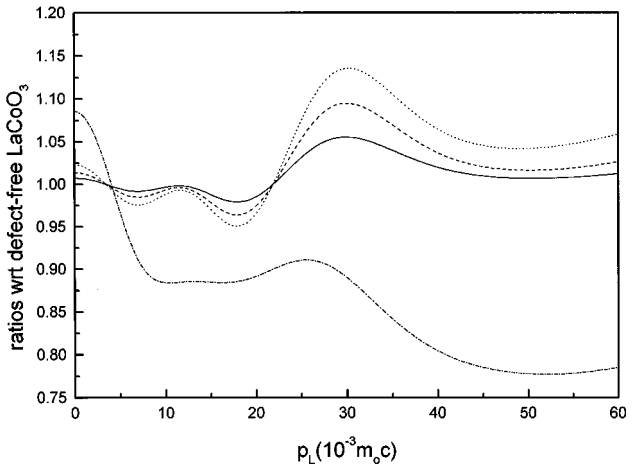

FIG. 5. Ratio curves for $La_{0.85}Si_{0.15}CoO_3$ (solid line), $La_{0.67}Sr_{0.33}CoO_3$ (dashed line), and $SrCoO_3$ (dotted line), and the $2Sr_{La}V_O$ complex with respect to defect-free $LaCoO_3$.

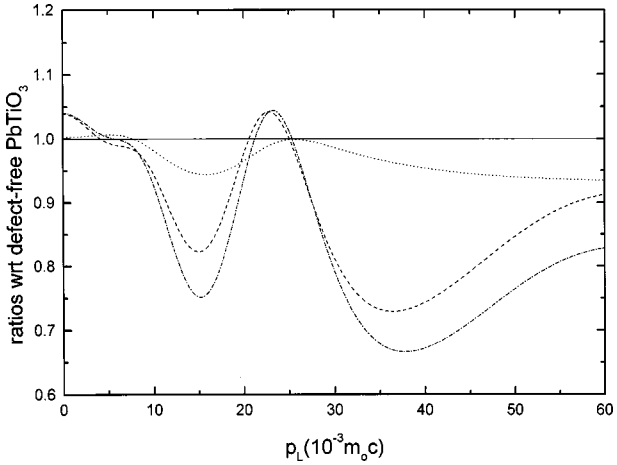

FIG. 6. Ratios of $PbTiO_3$ (solid line), $LaTiO_3$ (dashed line), $PbZrO_3$ (dotted line), and $LaZiO_3$ (dot-dashed line) with respect to defect-free $PbTiO_3$.

both Pb and Ti to create $LaZrO_3$. The ratio curves of all these hypothetical structures with respect to defect-free $PbTiO_3$ (Fig. 6) have very different features, and represent the maximum changes we expect to observe due to doping. Replacing all Pb atoms by La atoms results in a small decrease (11 ps) in the positron lifetime (Table II). If all Ti atoms are replaced by Zr atoms the calculations predict a 15 ps decrease in the lifetime, so it may not be possible to detect lifetime changes for small doping levels. Therefore, the changes in the shapes of the ratio curves (Fig. 6) due to doping may prove to be a better indicator of the presence of the sustitutional impurities.

When $BaTiO_3$ is doped with Sr, the Sr can occupy both Ba and Ti sites. The effect of Sr substitution is modeled by creating hypothetical $SrTiO_3$ and $BaSrO_3$ crystals with the same lattice constant as the $BaTiO_3$. When all Ba sites are occupied by Sr atoms there is a 12 ps increase in the positron lifetime (Table II). When all Ti sites are occupied by Sr atoms there is a 3 ps decrease in the positron lifetime. These changes in the lifetime are too small to be measured, especially for small variations in the doping concentration. The ratios of the Doppler profiles for the hypothetical $SrTiO_3$ and $BaSrO_3$ with respect to defect-free $BaTiO_3$ are plotted in Fig. 7. The two curves have very different shapes and these differences can be used to determine whether Sr occupies Ba or Ti sites.

When Sr^{2+} occupies Ti^{4+} sites it probably couples to an oxygen vacancy to form a charge-neutral defect complex. The calculated value of the positron lifetime associated with this defect (154 ps) was found to be somewhat lower than that for a simple oxygen vacancy (162 ps). The calculated ratio curve of the Doppler profile (Fig. 7) for this defect complex differs significantly from the ratio curves for the hypothetical crystals described above. However, the defect complex ($Sr_{Ti}V_O$) appears to have a ratio curve very similar to that of an isolated oxygen vacancy (Fig. 4), the main difference being that its high-momentum ($p_L > 30\times10^{-3}m_0c$) value is somewhat higher than that for a simple vacancy.

COMPARISONS WITH EXPERIMENT

Some positron lifetime measurements have been done on all these materials. The measurements for $La_{1-x}Sr_xCoO_3$ are

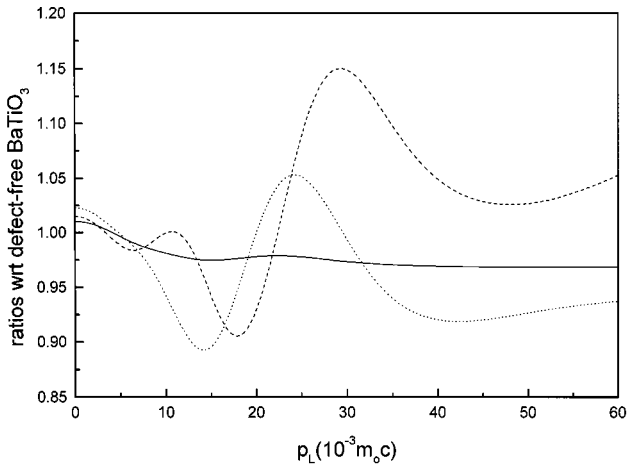

FIG. 7. Ratio curves for $BaTiO_3$ (dotted line), $SrTiO_3$ (dashed line), and the $Sr_{Ti}V_O$ complex (solid line) with respect to defect-free $BaTiO_3$.

discussed in Ref. 18, and they show the presence of two lifetimes in all samples. The bulk lifetime is found to be 138 ± 2 ps, and the Sr doping does not appreciably change the bulk lifetime. A longer lifetime, with an average value of 223 ± 10 ps can be resolved in all samples. This longer lifetime has been attributed to annihilations at single vacancies. For $x=0.5$ a new defect lifetime, which was not observed for samples with $0.0<x<0.05$, could be identified. This defect lifetime had a value of 149 ps, and was attributed to the presence of oxygen vacancies.

The positron lifetime measurements were repeated for the $x=0.05$ and $x=0.5$ samples after quenching from 1025 °C and 600 °C, respectively, to decrease the oxygen content. The lifetimes and intensities for the $x=0.5$ Sr-doped sample remained unchanged. The $x=0.05$ sample, which had shown no evidence of oxygen-related defects in the as-grown state, showed two defect lifetimes. These lifetimes were 157 ± 2 ps and 282 ± 3 ps. The shorter lifetime was attributed to the introduction of oxygen vacancies, and the larger lifetime to the formation of defect complexes consisting of metal and oxygen vacancies.

The calculated values of the positron lifetime (Table I) compare reasonably well with the measured values for the oxygen vacancies, but the lifetime calculated for the La vacancy (275 ps) is much larger than the measured value of 227 ps. The calculated values for site *A* vacancies in $PbTiO_3$ and $BaTiO_3$ are similar to those for the La vacancy, and the measured values are found to be larger than 300 ps.

Positron lifetimes have been measured in ferroelectric $BaTiO_3$ (Ref. 13) as a function of temperature and electric field, and in La-doped $BaTiO_3$ (Ref. 14) as a function of La doping. Two lifetime components were identified in ferroelectric $BaTiO_3$.[13] The shorter lifetime component of 160 ± 4 ps was associated with the bulk lifetime. The longer lifetime component varied between 318 and 347 ps as a function of temperature as well as of an electric field. On the basis of the temperature-dependent data the authors concluded that the longer lifetime was due to the Ba vacancies, and was strongly dependent on the crystal structure and Ti-O hybridization. The calculated value of the bulk positron lifetime in $BaTiO_3$ (Table I) is 152 ps, in good agreement with the experimental data. The calculated lifetime associated with the Ba vacancy is 293 ps, and this value is somewhat lower than the observed value. One possible explanation is that the experimentally observed lifetime results from Ba vacancies complexed with other vacancies.

In La-doped $BaTiO_3$ (Ref. 14) two lifetimes have been resolved, both of which vary with La doping. The shorter lifetime decreases from a value of 190 ps to ≈174 ps as the La concentration increases from 0 to 0.2 at %, and then increases to 210 ps as the La concentration increases further to 0.8 at .%. The value of the longer lifetime component follows the same trend, decreasing from 390 ps to 310 ps as the La concentration increases from 0 to 0.2 at .%, and then increasing to 420 ps as the La concentration increases further to 0.8 at .%. The authors argue that when the La^{3+} ions replace the Ba^{2+} ions two different charge compensation mechanisms can occur. The excess positive charge may be neutralized by Ti^{4+} changing to Ti^{3+} (electron compensation), or by the creation of Ba vacancies (vacancy compensation). The vacancy compensation mechanism would result in the creation of a defect complex consisting of $2La_{Ba}V_{Ba}$. The authors also conclude that the longer-lifetime component is an average lifetime due to positrons annihilating at isolated Ba vacancies and at grain boundaries, which may have a substantially larger lifetime. For further identification of defects in this case Doppler profile measurements may prove to be very useful.

Positron lifetimes have been measured for Bi-doped $Pb(Zr_{0.55}Ti_{0.45})O_3$, and La^{3+}-doped $PbTiO_3$.[15] The authors concluded that in La-doped $PbTiO_3$ the positrons annihilated at Pb vacancies, with a lifetime close to 304 ps. The defect-specific positron trapping rate into V_{Pb} was estimated to be 3.75×10^{-11} cm^3/s. The experimental lifetime of 304 ps is in good agreement with the calculated value of 280 ps for the Pb vacancy.

For the Bi-doped material, the trapping rate into vacancy-type defects increased with increasing dopant concentration, to a maximum value, and then started decreasing as dopant concentrations increased further. The trapping sites were assumed to be Pb vacancies for low Bi concentration. The authors concluded that as the Bi concentration increased the Bi atoms started occupying Ti or Zr sites. For the ABO_3 structure to remain electrically neutral when the Bi^{3+} occupied the Ti^{4+} or Zr^{4+} sites, O vacancies were created. These O vacancies formed a complex with a Pb vacancy to form a cation-anion vacancy pair, which may have a smaller defect-specific trapping rate than the isolated Pb vacancy. The positron results are in qualitative agreement with the results of the Goldschmidt factor analysis of Gonnard and Troccaz,[38] which shows that both *A* and *B* sites can be occupied by impurities, and that the distribution between the two sites depends on the ionic radius of the impurity. The large-radius Bi impurity will prefer the *A* (or Pb) site and will populate the *B* sites only when the dopant concentrations are larger. The lattice constant and cell volume of $Pb(ZrTi)O_3$ increase with an increase in the ratio of Zr/Ti, making it easier for the Bi ions to occupy the *B* sites.

CONCLUSIONS

Positron lifetimes and Doppler profiles have been calculated for a number of defects in $LaCoO_3$, $PbTiO_3$, and $BaTiO_3$. The effect of atomic relaxations on the positron lifetime at vacancies has been estimated. The calculated values of the positron lifetime have been compared to existing experimental data, and have been found to be in reasonably good agreement. To our knowledge Doppler profiles in metal oxides have not yet been measured. Our calculations show that the ratio curves of the Doppler profiles can be very useful in identifying defects in metal oxides. The ratio curves can also be used to determine which sublattice the vacancies and dopants occupy, and whether the dopants are complexed with any open-volume defects.

ACKNOWLEDGMENTS

This research was supported in part by the U.S. Department of Energy, Office of Basic Energy Sciences, Division of Materials Sciences under Contract No. DE-AC02-98CH10886. B.N. and T.F. acknowledge discussions with R. Ramesh, D.J. Keeble, and E.H. Poindexter, and financial support from the Materials Research Collaboration Program under US Army Contract No. DAAL01-95-2-3530.

[1] M. E. Lines and A. M. Glass, *Principles and Applications of Ferroelectric and Related Materials* (Clarendon, Oxford, 1977).
[2] MRS Bull. **21**, No. 7 (1996).
[3] D. M. Symth, J. Solid State Chem. **20**, 359 (1976).
[4] N. G. Eror and D. M. Symth, J. Solid State Chem. **24**, 235 (1978).
[5] R. K. Sharma, N.-H. Chan, and D. M. Symth, J. Am. Ceram. Soc. **64**, 448 (1981).
[6] Y. H. Hu, M. P. Harmer, and D. M. Symth, J. Am. Ceram. Soc. **68**, 372 (1984).
[7] *Positron Spectroscopy of Solids*, Proceedings of the International School of Physics ''Enrico Fermi,'' Course CXXV, Varena, 1993, edited by A. Dupasquier and A. P. Mills, Jr. (IOS, Ohmsha, 1995).
[8] T. McMullen, P. Jena, S. N. Khanna, Yi Li, and K. O. Jensen, Phys. Rev. B **43**, 10 422 (1991).
[9] K. O. Jensen, R. M. Nieminen, and M. J. Puska, J. Phys.: Condens. Matter **1**, 3727 (1989).
[10] G. H. Dai, P. W. Lu, X. Y. Huang, Q. S. Liu, and W. R. Xue, J. Mater. Sci.: Mater. Electron. **2**, 164 (1991).
[11] A. Chen and Y. Zhi, J. Appl. Phys. **71**, 4451 (1992).
[12] A. Chen and Y. Zhi, J. Appl. Phys. **71**, 6025 (1992).
[13] K. Süvegh, A. Domján, R. Tarsoly, and A. Vértes, J. Radioanal. Nucl. Chem. **211**, 255 (1996).
[14] C. Q. Tang, Phys. Rev. B **50**, 9774 (1994).
[15] Yuan-Jin He, Wei-Zhong Yu, Jia-Jiong Xiong, and Long-Tu Li, in *Positron Annihilation*, edited by P. C. Jain, R. M. Singru, and K. P. Gopinath (World Scientific, Singapore, 1985), p. 687.
[16] D. J. Keeble, B. Nielsen, A. Krishnan, K. G. Lynn, S. Madhukar, R. Ramesh, and C. F. Young, Appl. Phys. Lett. **73**, 318 (1998).
[17] D. J. Keeble, A. Krishnan, T. Friessnegg, B. Nielsen, S. Madhukar, S. Aggarwal, R. Ramesh, and E. H. Poindexter, Appl. Phys. Lett. **73**, 508 (1998).
[18] T. Friessnegg, S. Madhukar, B. Nielsen, A. R. Moodenbaugh, S. Aggarwal, D. J. Keeble, E. H. Poindexter, P. Mascher, and R. Ramesh, Phys. Rev. B **59**, 13 365 (1999).
[19] M. J. Puska and R. M. Nieminen, Rev. Mod. Phys. **66**, 841 (1994).
[20] P. A. Sterne and J. H. Kaiser, Phys. Rev. B **43**, 13 892 (1991).
[21] V. J. Ghosh, M. Alatalo, P. Asoka-Kumar, B. Nielsen, K. G. Lynn, A. C. Kruseman, and P. E. Mijnarends (unpublished); V. J. Ghosh, M. Alatalo, P. Asoka-Kumar, K. G. Lynn, and A. C. Kruseman, Appl. Surf. Sci. **116**, 278 (1997).
[22] A. Rubaszek, Z. Szotek, and W. M. Temmerman, Phys. Rev. B **58**, 11 285 (1999).
[23] M. Saito and A. Oshiyama, Phys. Rev. B **53**, 7810 (1996).
[24] M. Hakala, M. J. Puska, and R. M. Nieminen, Phys. Rev. B **57**, 7621 (1998).
[25] P. E. Mijnarends, A. C. Kruseman, A. van Veen, H. Schut, and A. Bansil, J. Phys.: Condens. Matter **10**, 10 383 (1998).
[26] B. Barbiellini, M. Hakala, M. J. Puska, R. M. Nieminen, and A. A. Manuel, Phys. Rev. B **56**, 7136 (1997).
[27] P. Asoka-Kumar, M. Alatalo, V. J. Ghosh, A. C. Kruseman, B. Nielsen, and K. G. Lynn, Phys. Rev. Lett. **77**, 2097 (1996); M. Alatalo, P. Asoka-Kumar, V. J. Ghosh, B. Nielsen, K. G. Lynn, A. C. Kruseman, A. van Veen, T. Korhonen, and M. J. Puska, J. Phys. Chem. Solids **59**, 55 (1998).
[28] M. Alatalo, H. Kauppinen, K. Saarinen, M. J. Puska, H. Makinen, P. Hautojarvi, and R. M. Nieminen, Phys. Rev. B **51**, 4176 (1995); M. J. Puska and R. M. Nieminen, Rev. Mod. Phys. **66**, 841 (1994).
[29] M. P. Petkov, M. H. Weber, K. G. Lynn, R. S. Crandall, and V. J. Ghosh, Phys. Rev. Lett **82**, 3819 (1999).
[30] V. J. Ghosh, B. Nielsen, A. C. Kruseman, P. E. Mijnarends, A. van Veen, and K. G. Lynn, Appl. Surf. Sci. **149**, 234 (1999).
[31] R. E. Cohen, Nature (London) **358**, 136 (1992).
[32] E. C. Subbarao and G. Shirane, J. Am. Ceram. Soc. **42**, 279 (1959).
[33] D. Hennings and K. H. Hardtl, Phys. Status Solidi A **8**, 465 (1970).
[34] A. N. Petrov, O. F. Kononchuk, A. V. Andreev, A. V. Cherepanov, and P. Kofstad, Solid State Ionics **80**, 189 (1995).
[35] R. C. Baetzold, Phys. Rev. B **38**, 11 304 (1988).
[36] J. D. Jorgensen, B. W. Veal, A. P. Paulikas, L. J. Nowicki, G. W. Crabtree, H. Claus, and K. W. Kwok, Phys. Rev. B **41**, 1863 (1990).
[37] V. J. Ghosh and D. O. Welch (unpublished).
[38] P. Gonnard and M. Troccaz, J. Solid State Chem. **23**, 321 (1978).